Catalysis Today 138 (2008) 135–140

Contents lists available at ScienceDirect

Catalysis Today

journal homepage: www.elsevier.com/locate/cattod

Zirconia-supported $LaCoO_3$ catalysts for hydrogen production by oxidative reforming of diesel: Optimization of preparation conditions

J.A. Villoria [a], M.C. Alvarez-Galvan [a,*], R.M. Navarro [a], Y. Briceño [b], F. Gordillo Alvarez [c], F. Rosa [d], J.L.G. Fierro [a]

[a] Instituto de Catálisis y Petroleoquímica (CSIC), Marie Curie 2, Cantoblanco, 28049 Madrid, Spain
[b] CIDAUT, Parque Tecnológico Boecillo, Valladolid, Spain
[c] Escuela Superior de Ingenieros, Sevilla, Spain
[d] Instituto Nacional de Técnica Aeroespacial (INTA), Centro de Experimentación de "El Arenosillo" (CEDEA), 21130 Huelva, Spain

ARTICLE INFO

Article history:
Available online 31 July 2008

Keywords:
Hydrogen production
ZrO_2-supported $LaCoO_3$
Oxidative reforming
Diesel

ABSTRACT

The influence of calcination temperature and precursor type used in the preparation of ZrO_2-supported $LaCoO_3$ catalyst on its behaviour for hydrogen production by oxidative reforming of diesel has been analyzed in terms of $LaCoO_3$ structure. Four samples have been prepared by wetness co-impregnation with cobalt and lanthanum salts and characterized by means of XRD, BET, SEM-EDX, TXRF and XPS. Physicochemical characterization shows a great influence of the nature of precursors and calcination temperature used in the synthesis on the textural, morphological, surface and structural properties of $LaCoO_3$ deposited over ZrO_2. The use of nitrate precursors and high calcination temperature leads to the formation of $LaCoO_3$ perovskite structures of high grain and crystallite size on ZrO_2 support. On the contrary, the catalyst prepared from acetate precursors and calcined at low temperature showed perovskite crystallites of lower size. For this sample, the smaller perovskite crystallites on the catalyst at the beginning of the reaction imply higher and more stable hydrogen production for short-term test aging test.

1. Introduction

The use of hydrogen in a fuel cell is an efficient and environmentally friendly power generation system compared to conventional combustion engines. One of the main ways to produce hydrogen is by reforming fossil fuels, being diesel a good alternative because of its high-energy density and well-established delivery infrastructure. Among the different catalytic processes to extract hydrogen from hydrocarbons existing in diesel, the oxidative reforming process, a combination of steam reforming and catalytic partial oxidation, has advantages respect to steam reforming and partial oxidation processes derived from its lower energy requirements and its better response to dynamic changes [1].

The successful extraction of hydrogen from diesel largely depends on the development of catalysts resistant to sulphur poisoning, coke formation, as well as to thermal sintering due to the high temperature reaction required in the process [2]. Although traditional catalysts based on supported noble or transition metals doped with thermal and activity promoters have been successfully used for this purpose [3], ABO_3 perovskite oxide systems are particularly suited catalysts precursors since they fulfil most of the above mentioned requirements [4,5]. Reduction of B-site cations in perovskite precursors under reaction atmosphere forms well-dispersed B metal particles in intimate contact with the A oxide which leads to high activity and also preventing carbon formation [5]. Among the different elements that can be used in the A position, lanthanum has found to have a positive influence in the catalyst stability improving coke gasification [6]. On the other hand, Co used as B-site element has shown an excellent performance as active metal for reforming processes [7]. However, the use of perovskite as catalyst precursors has an important drawback for the catalyst scale-up derived from the low surface area developed by perovskites. To circumvent this fact, pre-shaped structures such as foams [8] and silica–alumina fibers [9] have used as supports of perovskites. Podyacheva et al. [8] employed Ni and Ni–Cr foam substrates to deposit a $LaCrO_3$ perovskite phase. In both cases preliminary washcoating of the substrate was required in order to facilitate the anchorage of the perovskite phase. The supported perovskite was the only phase detected by diffraction methods and was stable up to calcination

* Corresponding author at: Instituto de Catálisis y Petroleoquímica (CSIC), Estructura y reactividad, Marie Curie 2, Cantoblanco, 28049 Madrid, Spain.
Tel.: +34 915 854773; fax: +34 915 854760.
E-mail address: c.alvarez@icp.csic.es (M.C. Alvarez-Galvan).

0920-5861/$ – see front matter © 2008 Elsevier B.V. All rights reserved.
doi:10.1016/j.cattod.2008.06.016

temperature of 1273 K. In another contribution, Klvana et al. [9] prepared NiCo-based perovskites supported on a commercial silica–alumina fibre blanket. The perovskite deposit (12–15%) was achieved by incipient wetting on the fiber blanket with the precursor solution, followed by fast freezing of the solution wet blanket by immersion in liquid nitrogen and vacuum drying. This system was particularly suitable for use in the combustion of lean natural gas mixtures and it exhibited activities comparable to those of commercial fibre-supported platinum and were found to be stable at temperatures below 1000 K.

The attempts of supporting $LaCoO_3$ systems over common substrates often find the problem of interactions between perovskite and the substrate. In the case of alumina substrates, solid state reactions usually take place between perovskite elements and supports involving the formation of aluminates and alumina spinels undesirable for an appropriate catalytic activity. As an example, previous experiments carried out in our laboratory trying to incorporate $LaCoO_3$ into alumina resulted in the formation of cobalt and lanthanum aluminates. Among common supports, Mizuno et al. [10] have reported the evolution of weak interactions between La or Co and the ZrO_2 support in $LaCoO_3$–ZrO_2 systems, concluding that it is possible to obtain a $LaCoO_3$ perovskite structures over ZrO_2 substrates.

In this scenario, in the present work we perform a study of the influence of $LaCoO_3$ incorporation method on ZrO_2 support with the aim to scale-up the preparation of reforming catalysts to be included in a diesel processor. The influence of different calcinations temperatures (823 or 1023 K) and cobalt and lanthanum precursors (acetates or nitrates) on the physicochemical properties of ZrO_2-supported $LaCoO_3$ samples has been studied, and correlated with the activity for hydrogen production by diesel oxidative reforming.

2. Experimental

The ZrO_2 support (zirconium oxide, catalyst support, 1/8 in. pellets, S_{BET} = 90 m^2/g, Johnson Matthey) was crushed and sieved to a particle size between 0.20 and 0.425 mm and stabilized by calcination at 1173 K for 6 h. $LaCoO_3$ was introduced into zirconia by wetness co-impregnation with aqueous solutions (0.8 M) of lanthanum nitrate (lanthanum (III) nitrate hexahydrate, 99.9% Johnson Matthey) and cobalt nitrate (cobalt (II) nitrate hexahydrate 98%, Sigma–Aldrich) or lanthanum acetate (La (III) acetate sesquihydrate, 99.9%, Ventron, Alfa produkte) and cobalt acetate (cobalt (II) acetate tetrahydrate, Sigma–Aldrich) (0.2 M in each because of the worse solubility of these Co and La precursors) in the appropriate ratio in relation with the amount of ZrO_2 to achieve 22 wt% $LaCoO_3$. After impregnation, the samples were dried at 383 K for 4 h and subsequently calcined in static air at 823 or 1023 K over 4 h using a temperature ramp rate of 1.2 and 1.8 K/min, respectively. The catalysts are designated as: A8, A10, N8 and N10 (“A” for those prepared from acetate and “N” from nitrate precursors; “8” for calcination at 823 K and “10” for calcination at 1023 K).

Elemental analysis was performed by total reflection X-ray fluorescence (EXTRA-2 Rich & Seifert) (TXRF). The BET surface area of the catalyst samples was calculated from the nitrogen adsorption/desorption isotherms. These isotherms were determined at the liquid nitrogen temperature (77 K) using a Micromeritics ASAP 2100 automatic equipment. The morphology of the fresh catalysts was analyzed by a scanning electron microscope (Hitachi S-3000N) coupled with an energy dispersive X-ray analyzer (INCAx-sight, Oxford Instruments). Acceleration voltage was 20 kV. The samples were dispersed on an aluminum stub and coated with Au film. XRD patterns were recorded using a Seifert 3000P vertical diffractometer and nickel-filtered Cu Kα radiation (λ = 0.1538 nm). The mean $LaCoO_3$ particle size was then estimated from X-ray line broadening using the Scherrer equation. Width was taken as the full width at half maximum intensity of the most intense and least overlapped peak (2θ = 47.5°).

XPS measurements were recorded using a Escalab 200R spectrometer equipped with a hemispherical electron analyzer and an Al Kα ($h\cdot\nu$ = 1486.6 eV) 120 W X-ray source. The area of the peaks was estimated by calculating the integral of each peak after smoothing and subtraction of a S-shaped background and fitting of the experimental curve to a mixture of Lorentzian and Gaussian lines of variable proportions. All binding energies (BE) were referenced to the C 1s signal at 284.6 eV from carbon contamination of the samples to correct the charging effects. Quantification of the atomic fractions on the sample surface was obtained by integration of the peaks with appropriate corrections for sensitivity factors.

Activity tests were performed at atmospheric pressure in a fixed-bed reactor at GHSV = 100,000 h^{-1}, H_2O/C = 3, O_2/C = 0.5 and 1123 K. Diesel has been provided by CEPSA (R&D Center) and its sulphur amount was 12 ppm. The catalyst was diluted with SiC (dp = 0.5 mm; SiC/catalyst = 5 vol.) to avoid preferential gas flow parts and hot spots. Prior to each run, the catalysts were pretreated in situ under flowing nitrogen (15 N mL/min) up to the reaction temperature (1123 K). The reaction stream was analyzed on line by a HP 5890 Series II equipped with two columns (4A Molecular Sieve and Porapack N (80/100) with a TC detector which was programmed to operate under high-sensitivity conditions. The molecular sieve was used to analyze H_2, O_2, N_2, CO and CH_4 and the packed column to analyze CO_2, C_2H_4, C_2H_6 and H_2O. Nitrogen was used as an inert standard for quantification. The hydrogen yield was expressed as % extracted hydrogen with respect to the maximum amount (mol) that can be produced from oxidative reforming of diesel hydrocarbons, assuming complete conversion to CO_2 and hydrogen. A chemical analysis of diesel (Elemental analyzer, LECO CHNS-932) showed an average chemical formula of $C_{14.4}H_{27.2}$.

3. Results and discussion

Precursor type and calcination temperature used in the preparation of the different ZrO_2-supported $LaCoO_3$ samples as

Table 1
BET surface area, mean $LaCoO_3$ particle size (Scherrer), Co/La and Co/La + Zr ratios for fresh ZrO_2-supported $LaCoO_3$ catalysts

Catalyst	Co and La precursors	Calcination temperature (K)	A_{BET} (m^2/g)	Mean $LaCoO_3$ particle ize (nm)		Atomic ratios (TXRF)		Surface atomic ratio by weight unit (XPS)		
				Fresh	Pretreated	Co/La	Co/(La + Zr)	Fresh	Used	
								Co/(La + Zr)	Co/La	Co/(La + Zr)
A8	Acetates	823	11	16	18	0.88	0.23	1.86	1.82	0.65
A10	Acetates	1023	12	36	35	0.63	0.15	0.62	0.49	0.30
N8	Nitrates	823	7	23	37	0.99	0.38	3.54	0.76	0.32
N10	Nitrates	1023	6	40	43	0.96	0.36	1.16	1.02	0.84

well as their main physicochemical characteristics are summarized in Table 1. A decrease in specific BET area with respect to the bare calcined zirconia (16 m^2/g) is observed for all the samples. The drop in BET area is more pronounced for the samples prepared using nitrate precursors.

Fig. 1 shows perovskite grains derived from SEM analysis carried out over fresh catalysts. Perovskites of different grain morphology were produced depending on both the type of Co- and La-precursors and the calcination temperature used in the synthesis. SEM images show that the grain size is around 0.1–0.3 μm, being larger and more defined for samples prepared from nitrate precursors (N8 and N10, Fig. 1). It can also be observed some grain agglomeration. Although zirconia support has also a role in the obtained BET area, the smaller mean grain size found for samples prepared from acetate precursors should be involved with the increase in surface area observed.

The effect of precursor type in the morphology of $LaCoO_3$ grains, may be influenced by the isolectric point of zirconia (4) and the different pHs of acetate (around 9) and nitrate (around 5) solutions. In both cases the support surface will be negatively charged. However, the negative charge will be higher for acetate solution, therefore favouring the spreading of cobalt and lanthanum cations over the ZrO_2 surface. Greater dispersion of supported cobalt when acetate precursor is used instead of nitrate has been reported in the literature [11].

XRD patterns of fresh and pretreated $LaCoO_3/ZrO_2$ samples (Fig. 2) show diffraction lines corresponding to rhombohedral $LaCoO_3$ (JC-PDS 84-848), monoclinic ZrO_2 (JC-PDS 83-944), Co_3O_4 (JC-PDS 76-1802) and La_2O_3 (JC-PDS 22-369). Moreover, some phases attributed to the incomplete decomposition of lanthanum acetate (La_2CO_5) (JC-PDS 23-322) or nitrate ($La_5O_7NO_3$) (JC-PDS 38-891) during calcination are observed in the patterns of fresh samples calcined at lower temperature (A8 and N8 in Fig. 2). All the intermediates from precursors transform into La_2O_3 when treated at 973 K or above [12]. It is important to notice that there is no loss of active phases by strong interaction with the ZrO_2 support since any cobalt or lanthanum zirconates are not observed; in this sense, the benefit of using zirconia-based supports to increase $LaCoO_3$ formation is confirmed.

The diffraction patterns in Fig. 2 show a higher intensity in $LaCoO_3$ diffraction lines and the formation of bigger $LaCoO_3$ particles for systems prepared using nitrate precursors (Table 1). For the same calcination temperature, smaller $LaCoO_3$ particles are formed in both fresh and pretreated catalysts prepared from acetate precursors. For the same precursor, the presence of better crystallized perovskite structure become more evident with the increase in the calcination temperature [13] as indicate the increase in perovskite crystallite mean size (Table 1). On the other hand, the cobalt spinel peaks present lower intensity for samples prepared from acetate precursors (Fig. 2) indicating a greater incorporation of cobalt to perovskite structure. Pretreatment under inert only produces a substantial increase in $LaCoO_3$ particle size for the sample prepared from nitrate precursors and calcined at lower temperature (N8, Table 1).

Fig. 3 shows the Co 2p photoelectron spectra of the $LaCoO_3/ZrO_2$ fresh systems. For A10 and N10 samples, the binding energy values (lesser than 780 eV), and shape of XPS profiles (without the presence of a satellite in the Co 2p signal) indicate the presence of $LaCoO_3$ on the surface [14,15]. In the case of A8 and N8 samples, the satellite band that appears at 789 eV indicates the surface contribution of Co_3O_4 species. This fact may be derived from a calcination temperature not high enough to incorporate all cobalt phase into perovskite structure, thus forming some cobalt oxide particles in the surface [16].

The La 3d level is characterized by a double peak for each spin–orbit component, attributed to energy loss phenomena (shake-up satellites) induced by intense O 2p → La 4f charge transfer events or to strong final state mixing of electronic configurations [17]. The

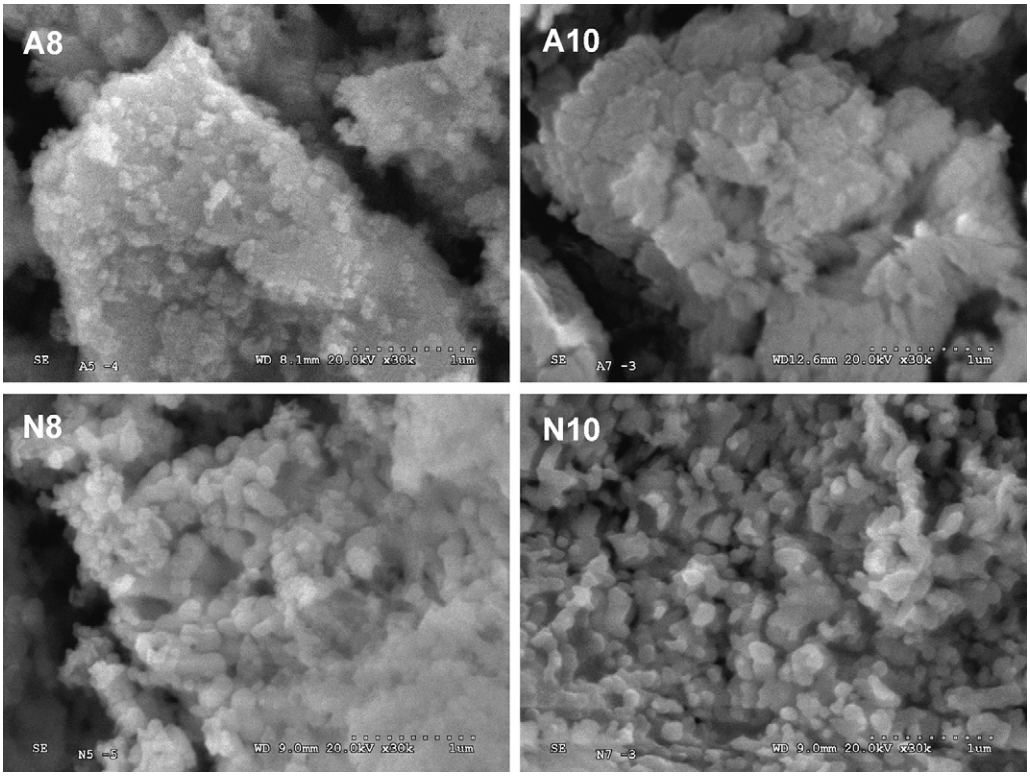

Fig. 1. Scanning electron microscopy images for fresh catalysts.

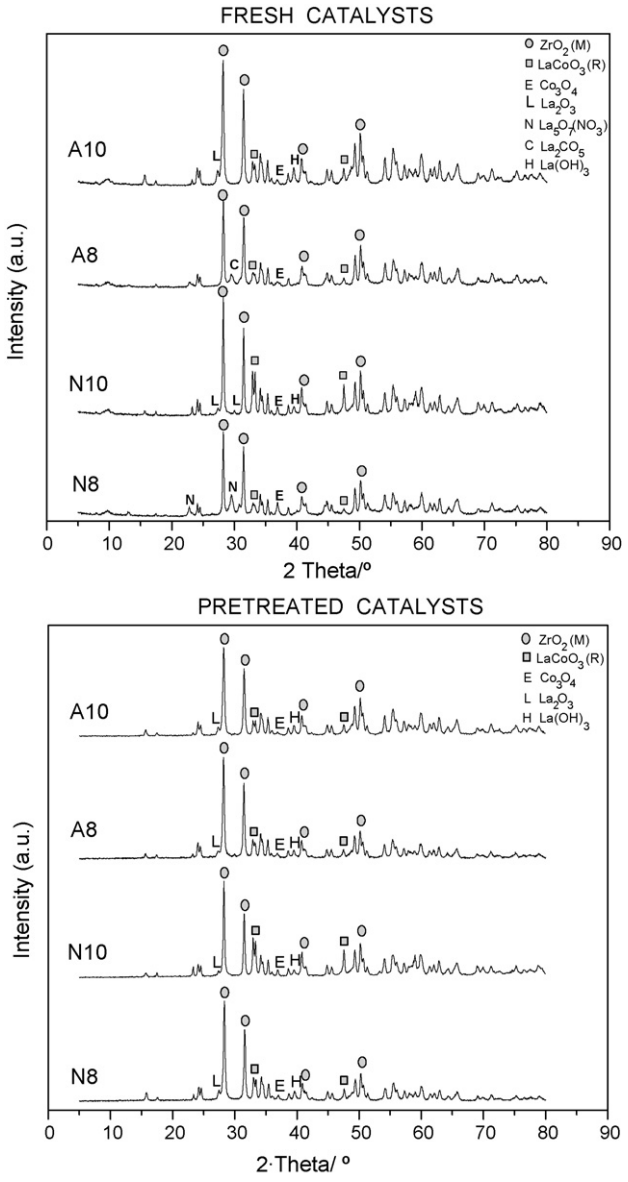

Fig. 2. X-ray diffraction patterns for fresh and pretreated catalysts.

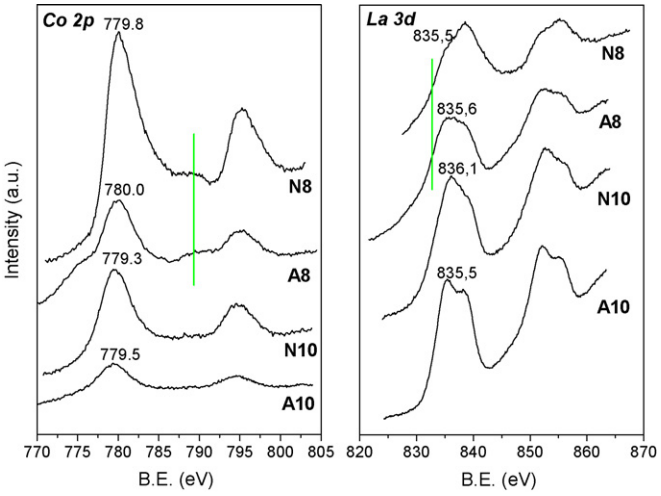

Fig. 3. Co 2p and La 3d photoelectron spectra for fresh catalysts.

binding energies, the similarities of intensities and the energy separations for both peaks, that give to not well resolved profiles, show mainly the presence of $LaCoO_3$ in the surface of all the samples [18]. For samples calcined at lower temperature, A8 and N8, La $3d_{5/2}$ peak exhibits a component around 833–834 eV that increases the wide of this peak. This comes from a thin layer of lanthanum carbonate not incorporated to $LaCoO_3$ perovskite structure during the synthesis. This interpretation is consistent with the observation of a C 1s line at a binding energy of 288.6 eV which is characteristic of carbonate species and with some carbonate compounds observed by XRD for above samples. The formation of carbonate species is rather usual in lanthanide oxides because of their strong tendency toward atmospheric carbon dioxide adsorption and formation of stable surface carbonates [19,20]. Finally, the Zr 3d spectra exhibited line profile typical of ZrO_2, with binding energy of the most intense Zr $3d_{5/2}$ peak with maxima centered at 182.2–182.5 eV.

Quantitative surface composition of the samples was also determined. Surface atomic ratios were calculated from the intensities of La 3d, Zr 3d, and Co 2p peaks and taking into account the sensitivity factors given by Wagner et al. [21]. Results of surface compositions derived from XPS data along with the results of chemical analysis by TXRF are given in Table 1. The Co/La values obtained from TXRF are similar to that expected from nominal loading, except for A10 sample that gives a lower value. The differences in Co/(La + Zr) ratio between the bulk and the surface catalyst composition are associated with the impregnation method used to introduce La and Co phases over zirconia-support. In relation to XPS surface values, a decrease in Co/(La + Zr) ratio with calcination temperature for both type of active phases precursors is observed. The drop of Co/(La + Zr) surface ratio is attributed to the formation of perovskite crystallites with high particle size, that produce more ZrO_2-free surface upon the growth of $LaCoO_3$ particles, which is in harmony with the XRD data as commented above. The high value of this ratio measured for N8 sample can be associated to the greater extent of cobalt oxide spinel developed on its surface. Although the surface exposure of cobalt species is essential for the catalytic behaviour, it should be also stressed that the role of both lanthana and zirconia to activity and stability may also be important. A certain surface exposition of each component in relation to the others is crucial to obtain high and stable hydrogen production. Thus, it has been reported the

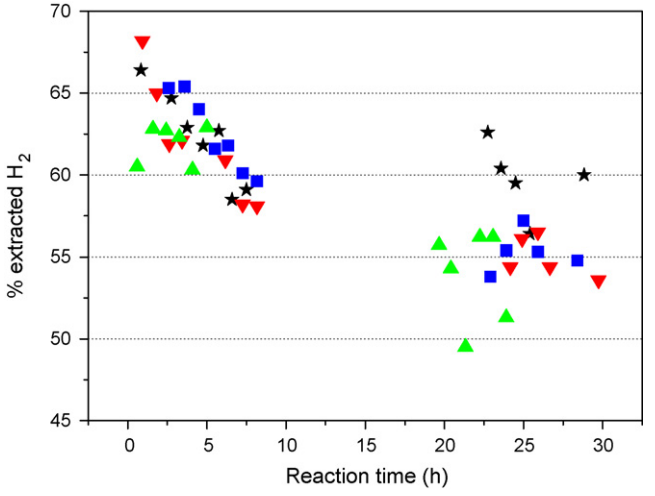

Fig. 4. Hydrogen yield for ZrO_2-supported $LaCoO_3$ catalysts (GHSV = 100,000 h^{-1}, $H_2O/C = 3$, $O_2/C = 0.5$ and 1123 K) (A8, ★; A10, ▼; N8, ▲; N10 ■).

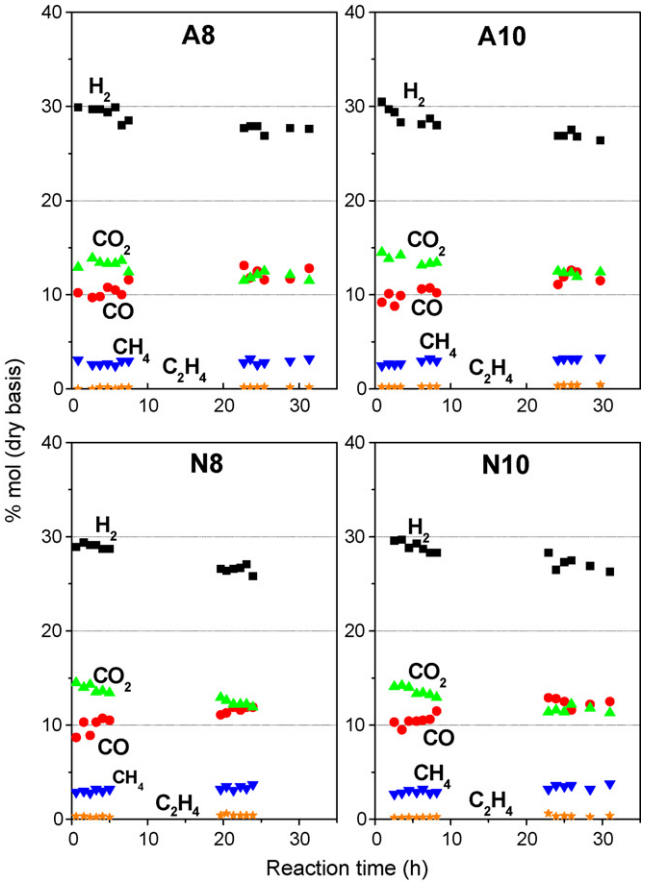

Fig. 5. Product distribution for ZrO_2-supported $LaCoO_3$ catalysts (GHSV = 100,000 h^{-1}, $H_2O/C = 3$, $O_2/C = 0.5$ and 1123 K).

ability of zirconia [22] and lanthana [5] to activate CO_2 adsorption, promoting the gasification of carbon precursors.

Diesel conversion obtained for all the catalysts is 100% at the beginning of reaction and decreases less than 5% after 24 h on-stream. As shown in Fig. 4, the yields toward hydrogen are very close for all the catalysts in the first hours of reaction. The H_2 yield increases with time for catalyst N8 because is being reduced by the feed. This reduction of perovskite produces metallic cobalt over a lanthana matrix, the real catalyst for this process, thus the yield increases with the proportion of the reduced phase in the catalytic bed. This fact does not happen in the other three systems since they were reduced during activation by the action of rests of hydrocarbons present in the vaporizer. Hydrogen yield decreases with time on-stream for catalysts A8, A10 and N10 in the first 8 h of reaction. It is also observed a decrease in activity of the second series of analysis in relation with the first one for all the systems. Factors responsible for this drop in activity can be: (i) sintering and/or volatilization of metallic cobalt; (ii) coke deposition on the metallic particles; and (iii) sulphur poisoning [23]. From these factors, sintering and/or volatilization of small cobalt active particles are those that seem to affect more in the first hours of reaction. XPS analysis of used catalysts (Table 1) show a decrease in cobalt surface exposition for all the samples in relation with values obtained for fresh sample which is in accordance with the deactivation observed in the first hours of reaction. Carbon deposition on used catalysts was determined by CHNS elemental analysis, being not found differences of importance between the analyzed samples, with concentrations between 2 and 3 wt% for all the samples. Sulphur content on all used samples, also determined

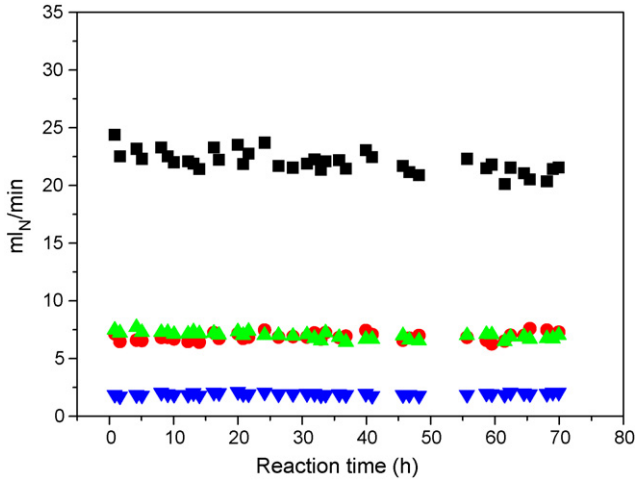

Fig. 6. Yields to different products for catalyst A8 in a long-term test (GHSV = 20,000 h^{-1}, $H_2O/C = 3$, $O_2/C = 0.5$ and 1123 K) (H_2, ■ ; CO, ●; CO_2, ▲; CH_4, ▼).

by CHNS elemental analysis was very low with a concentration lesser than 0.05 wt%.

Fig. 4 also shows that the La–Co/ZrO_2 catalyst prepared with acetate precursors and calcined at lower temperature (A8) displays some higher hydrogen yield. Although, there is some spread in the data, as a whole, and comparing mean hydrogen yields values, it can be observed some higher hydrogen production (around 10%) for catalyst A8. In relation with CO_2 formation, this product decreases in the first 25 h of reaction for all the catalysts. This fact is joined with an increase in the formation of CO (Fig. 5) which indicates the development of the reverse water–gas shift reaction. It is also observed the formation of some hydrogen-containing molecules such as methane and ethylene. Obtained product compositions are similar to that found in the literature in a diesel fuel processor using as catalyst Pt-supported on modified alumina [24] although some lower for hydrogen production. However, taking into account the high space velocity used in our experiments, zirconia-supported catalysts prepared seem very promising to be scaled up. Thus, product compositions are comparable to those obtained in an autothermal reformer for hydrogen production from heavy hydrocarbons [25], in which is used a commercial monolithic catalyst made of cordierite with a washcoat of cerium oxide and gadolinium oxide with 1% Pt using similar operation conditions.

A8 catalyst has been subjected to eight cycles of 8 h of reaction each and only a slight deactivation has been observed after the first 25 h (Fig. 6). This better catalytic performance may be caused by the formation of smaller grain size and crystallites of perovskite being more able to develop finely dispersed metal cobalt phase, along with the higher Co/La ratio found for this catalyst (Table 1), thus improving activity and coke gasification by the action of lanthanum oxycarbonate [7].

4. Conclusion

A successful preparation of zirconia-supported $LaCoO_3$ catalyst, in which no loss of active phases has occurred by interaction with support during the synthesis, as confirmed by XRD and XPS, has been achieved since no formation of cobalt or lanthanum zirconiates has been evidenced.

$LaCoO_3$-supported on ZrO_2 catalyst prepared from acetate precursors and calcined at 823 K, with smaller perovskite grain size and smaller $LaCoO_3$ crystallites, has been found to be very

active and stable for hydrogen production by oxidative reforming of diesel, even at very high space velocities, respect to those calcined at higher temperature or prepared from nitrate precursors. This methodology of synthesis improves the textural and mechanical properties of $LaCoO_3$ and seems suitable with a view to scale-up the catalyst for its use in diesel reformers.

Acknowledgements

This work was carried out within the framework of the Project "Development of a Diesel fuel processor" carried out at INTA, CIDAUT, AICIA and ICP (CSIC). MCA-G acknowledge financial support from the MCYT in the Ramon y Cajal research program.

References

[1] P.K. Cheekatamarla, A.M. Lane, J. Power Sources 152 (2005) 256.
[2] A.F. Ghenciu, Curr. Op. Sol. St. Ma. Sci. 6 (2002) 389.
[3] M.C. Alvarez-Galvan, R.M. Navarro, F. Rosa, Y. Briceño, F. Gordillo Alvarez, J.L.G. Fierro, Int. J. Hydrogen Energy 33 (2008) 652.
[4] M.A. Peña, J.L.G. Fierro, Chem. Rev. 101 (2001) 1981.
[5] R. Lago, G. Bini, M.A. Peña, J.L.G. Fierro, J. Catal. 167 (1997) 198.
[6] Z.L. Zhang, X.E. Verykios, Appl. Catal. A: Gen. 138 (1996) 109.
[7] R.M. Navarro, M.C. Alvarez-Galvan, J.A. Villoria, I.D. Gonzalez-Jimenez, F. Rosa, J.L.G. Fierro, Appl. Catal. B: Environ. 73 (2007) 247.
[8] O.Y. Podyacheva, A.A. Ketov, Z.R. Ismagilov, V.A. Ushakov, A. Bos, H.J. Veringa, React. Kinet. Catal. Lett. 60 (1997) 243.
[9] D. Klvana, J. Kirchnerova, J. Chaouki, J. Delval, W. Yaici, Catal. Today 47 (1999) 115.
[10] N. Mizuno, H. Fujii, H. Igarashi, M. Misono, J. Am. Chem. Soc. 114 (1992) 7151.
[11] M. Kraum, M. Baerns, Appl. Catal. A: Gen. 186 (1999) 189.
[12] L. Fabbrini, I. Rossetti, L. Forni, Appl. Catal. B: Environ. 56 (2005) 221.
[13] S. Cimino, R. Pirone, L. Lisi, Appl. Catal. B: Environ. 35 (2002) 243.
[14] E.A. Lombardo, K. Tanaka, I. Toyoshima, J. Catal. 80 (1983) 340.
[15] E. Bontempi, L. Armelao, D. Barreca, L. Bertolo, G. Bottaro, E. Pierangelo, L.E. Depero, Cryst. Eng. 5 (2002) 291.
[16] H.A.E. Hagelin-Weaver, G.B. Hoflund, D.A. Minahan, G.N. Salaita, Appl. Surf. Sci. 235 (2004) 420.
[17] M.N. Natile, E. Ugel, C. Maccato, A. Glisenti, Appl. Catal. B: Environ. 72 (2007) 351.
[18] R.P. Vasquez, Phys. Rev. B 54 (1996) 14938.
[19] M.P. Rosynek, D.T. Magnuson, J. Catal. 48 (1977) 417.
[20] S. Ponce, M.A. Peña, J.L.G. Fierro, Appl. Catal. B: Environ. 24 (2000) 193.
[21] C.D. Wagner, L.E. Davis, M.V. Zeller, J.A. Taylor, R.H. Raymond, L.H. Gale, Surf. Inter. Anal. 3 (1981) 211.
[22] F. Pompeo, N.N. Nichio, O.A. Ferretti, D. Resasco, Int. J. Hydrogen Energy 30 (2005) 1399.
[23] D. Liu, M. Krumpelt, Presentation at SECA Diesel Fuel Processing Workshop, Pittsburgh, 2005.
[24] D. Sopeña, A. Melgar, Y. Briceño, R.M. Navarro, M.C. Álvarez-Galván, F. Rosa, Int. J. Hydrogen Energy 32 (2007) 1429.
[25] D. Liu, T.D. Kaun, H. Liao, S. Ahmed, Int. J. Hydrogen Energy 29 (2004) 1035.